

Anisotropy, Itineracy, and Magnetic Frustration in High- T_C Iron Pnictides

Myung Joon Han, Quan Yin, Warren E. Pickett, and Sergey Y. Savrasov

Department of Physics, University of California, Davis, California 95616, USA

(Received 31 October 2008; published 11 March 2009)

Using first-principles density functional theory calculations combined with insight from a tight-binding representation, dynamical mean field theory, and linear response theory, we have extensively investigated the electronic structures and magnetic interactions of nine ferropnictides representing three different structural classes. The calculated magnetic interactions are found to be short range, and the nearest (J_{1a}) and next-nearest (J_2) exchange constants follow the universal trend of $J_{1a}/2J_2 \sim 1$, despite their itinerant origin and extreme sensitivity to the z position of As. These results bear on the discussion of itineracy versus magnetic frustration as the key factor in stabilizing the superconducting ground state. The calculated spin-wave dispersions show strong magnetic anisotropy in the Fe plane, in contrast with cuprates.

DOI: 10.1103/PhysRevLett.102.107003

PACS numbers: 74.70.-b, 71.20.-b, 75.25.+z, 75.30.-m

Recent discovery of the new high-temperature superconductor, $\text{LaO}_{1-x}\text{F}_x\text{FeAs}$ with a transition temperature (T_C) of 26 K [1] has triggered tremendous research activities on iron pnictides. Rare-earth (RE) doping increases T_C up to 55 K for Sm [2,3]. Replacing RE-O layers with Li produces an intrinsic superconductor LiFeAs with T_C of 18 K [4]. The 122 ferropnictides, ALFe_2As_2 (AL: Ca, Sr, Ba, K), span another structural class with T_C up to 38 K [5–10]. More recently, arsenic-free $\text{FeSe}_{1-\delta}$ and $\text{Fe}(\text{Se}_{1-x}\text{Te}_x)_{1-\delta}$ without any interlayer between Fe-(Se,Te) planes were found to be superconducting at T_C as high as 27 K under pressure [11–14]. In spite of the accumulating reports of both experiments and theories, the nature of the superconductivity and magnetism is still far from clear. After several works have ruled out the electron-phonon coupling [15,16], and the coexistence of magnetic fluctuation and superconductivity being confirmed by muon spin rotation (μSR) [17], intensive investigations have been focused on the magnetic properties of these systems [18–25]. From the studies up to now, one of the common and evident features is the interplay between superconductivity and magnetism. It is clear, from the different structures, that the essential physics lies in the iron plane forming the two-dimensional spin lattice.

Except for the Fe(Se,Te) family suggested to have different magnetic structures by recent studies [18–20], it is widely believed that the first three classes of Fe pnictides have a common superconducting mechanism closely related to magnetic interactions. In order to clarify the raised issues and lead to further understanding, it is of key importance to investigate the exchange interactions across different classes of compounds and examine any trend or common features. However, material-specific information of magnetic interactions is scarce in spite of active research efforts. The direct probe of spin dynamics is inelastic neutron scattering [9,26,27] which revealed that the combination of nearest- and next-nearest-neighbor exchange interactions $|J_{1a} + 2J_2|$ is about 100 meV, but detailed data from individual contributions, as well as their anisotropy

and the proximity of the ratio $J_{1a}/2J_2$ to unity, which has been discussed extensively in recent publications [21–23], are still missing.

In this Letter, using first-principle linear response calculations [28,29], we provide the data of in-plane magnetic exchange couplings for several Fe-based superconductors, and discuss their spin-wave dispersions. The data bear on the question of whether the values of exchange constants indicates magnetic fluctuations play an important role. A total of nine materials have been studied: REFeAsO (RE: La, Ce, Pr, Nd), ALFe_2As_2 (AL: Ca, Sr, Ba, K), and LiFeAs . Exchange interactions of these systems are found to be short range despite the metallic density of states (DOS), and the calculated interaction strengths follow the universal behavior of $J_{1a} \approx 2J_2$ for all materials, a relation that arises independently in the frustrated magnetic picture [21–23]. Considering not only the variety of the materials studied here but also the high sensitivity of the Fe moment to the z position of As atom [30,31], this universal behavior of the exchange interactions is impressive. The calculated spin-wave dispersion shows an anisotropic spin interaction which is different from the cuprates.

There have been several published tight-binding (TB) parametrizations of the electronic structure of prototypical LaFeAsO in the vicinity of the Fermi level using fits based either on Wannier functions or atomic basis sets [32–35]. However, the current situation still looks complicated because the projected DOS deduced from electronic structure calculations are based on the spherical harmonic projectors within the atomic spheres that may not be very well suited for the extended Fe and As orbitals presented here. Because of these complications even the crystal field splitting of Fe d level appears to be controversial in the current literature [32–35].

To better understand the complicated electronic structure around Fermi level, we performed TB analysis by considering d_{xz} and d_{yz} orbitals of Fe t_{2g} manifold hybridizing with the arsenic p_x and p_y , respectively. As shown in Fig. 1, the separation between the energy levels of Fe- t_{2g}

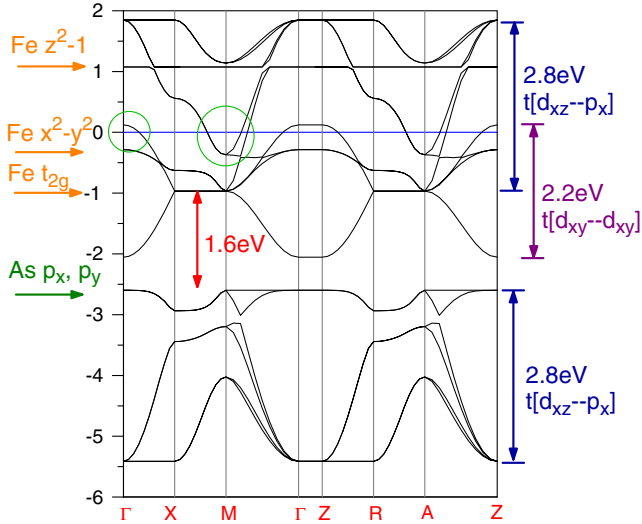


FIG. 1 (color online). The tight-binding band structure of LaFeAsO. The circles at the Fermi level on the Γ and M points indicate the hole and electron pockets, respectively.

and As- $p_{x,y}$ states is about 1.6 eV. Accounting for the hybridization matrix element between $d_{xz}-p_x$, $d_{yz}-p_y$ states, which is of the order of 1.8 eV, produces bonding and antibonding bands, both having the bandwidth of 2.8 eV with the Fermi level falling into the antibonding part of the spectrum (approximately 1 eV above the Fe t_{2g} level). We also take into account the d_{xy} state of Fe which hybridizes with itself (hopping integral is approximately 0.3 eV), which produces an additional bandwidth of 2.2 eV. The resulting bandwidth of Fe d -electron character near the Fermi level becomes $2.8 + 2.2/2 = 3.9$ eV as exactly seen in the local density approximation (LDA) calculation [36]. The coordinate system used for this TB description is the original crystallographic lattice where the spin alternates in the (π, π) direction. In this picture, the Γ -centered hole pockets (small circle in Fig. 1) are mostly of d_{xy} character, and the M -centered pockets (large circle) are of d_{xz} , d_{yz} character. This picture can be fine-tuned further by including the $d_{x^2-y^2}$ state which lies 0.3 eV below the Fermi level and hybridizes primarily with As- $p_{x,y}$ states (hopping integral is about 0.8 eV) as well as hybridization between $d_{xz,yz}$ orbitals with As p_z states (hopping integral is about 0.4 eV). Note that in this picture the Fe d_{z^2-1} orbital becomes unoccupied and lies 1 eV above the Fermi level.

Now we discuss the exchange interactions. To calculate the interactions between Fe moments, we used linear response theory [37,38] based on first-principle density functional theory (DFT) calculations, which has been successfully applied to the 3d transition-metal oxides and the 5f actinides metallic alloys [38,39]. We used the full potential linearized muffin-tin orbital as the basis set [40] and local spin density approximation (LSDA) for the exchange-correlation energy functional. The LSDA is fairly good in describing the itinerant Fe 3d states in these materials as shown in the previous studies and comparisons

with angle resolved photoemission [30,31,36,41]. In the calculations of REOFeAs compounds, we used the LSDA + DMFT (where DMFT represents dynamical mean field theory) method [28,29] in which the RE 4f orbitals are treated as the localized ones within Hubbard I approximation. $U = 6$ eV and $J_H = 0.86$ eV were used as the on-site Coulomb repulsion and Hund's rule exchange parameter. Lattice constants are taken from experiments, and we performed the calculations at various $z(\text{As})$, including experimental $z(\text{As})_{\text{exp}}$ and LDA-optimized $z(\text{As})_{\text{LDA}}$.

Figure 2 shows the spin structure of the Fe plane which is common to the all these materials. From here on we use the $(\pi, 0)$ striped antiferromagnetic (AFM) coordinate system, which is convenient to discuss the spin-wave dispersions. Magnetic interactions between Fe moments are governed by two dominating AFM couplings J_{1a} and J_2 , and the ferromagnetic (FM) nearest-neighbor exchange J_{1b} is small. We found the exchange couplings $J(\mathbf{q})$ can be expressed in terms of short-range exchange constants. This character suggests pursuing a comparison with local moment models with AFM spin interactions [21–23]. The short-range couplings do not conflict with the itinerant magnet picture because although the Fe 3d orbital has finite DOS at the Fermi level, the magnetic interactions can still remain short range, which possibly reflects the bad metallicity and some correlation effects.

The calculated Fe magnetic moments and exchange interactions are summarized in Table I. We use the convention that positive J means AFM couplings. The calculated moments are consistent throughout the materials. The calculations done at experimental $z(\text{As})_{\text{exp}}$ are known to predict the moments about twice as large as experimental values, while at optimized $z(\text{As})_{\text{LDA}}$ they give smaller moments. The cases in which DFT overestimates magnetic moments are rare, and the cause is still under debate. Although some theorists suggest it is due to the frustrated magnetic structure [21], Mazin and Johannes suggest an alternative picture [42] based on magnetic fluctuation and inhomogenities. Importantly, the electronic structure features such as electron-hole symmetry and the exchange interaction strengths are better described with $z(\text{As})_{\text{exp}}$ when compared to available experimental data [9,26]. Thus our discussion will be based on the results from

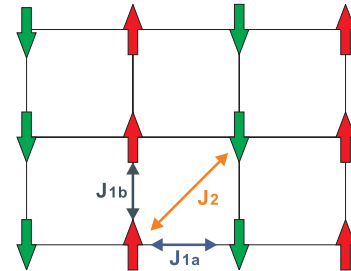


FIG. 2 (color online). Spin arrangement and exchange interactions in the Fe plane of the striped Q_m -AFM phase.

TABLE I. Calculated Fe moments (in μ_B) and in-plane exchange interactions (in meV), using experimental $z(\text{As})$.

System	Moment	J_{1a}	J_2	J_{1b}	$J_{1a}/2J_2$	$J_{1a} + 2J_2$
LaFeAsO	1.69	47.4	22.4	-6.9	1.06	92.2
CeFeAsO	1.79	31.6	15.4	2.0	1.03	62.4
PrFeAsO	1.76	57.2	18.2	3.4	1.57	93.6
NdFeAsO	1.49	42.1	15.2	-1.7	1.38	72.5
CaFe ₂ As ₂	1.51	36.6	19.4	-2.8	0.95	75.4
SrFe ₂ As ₂	1.69	42.0	16.0	2.6	1.31	74.0
BaFe ₂ As ₂	1.68	43.0	14.3	-3.1	1.51	71.5
KFe ₂ As ₂	1.58	42.5	15.0	-2.9	1.42	72.5
LiFeAs	1.69	43.4	22.9	-2.5	0.95	89.2

$z(\text{As})_{\text{exp}}$. The sensitivity of moments and exchange interactions to $z(\text{As})$ is large. For example, in LaFeAsO the change of $z(\text{As})$ by 0.04 \AA [$\Delta z(\text{As}) = 0.005$ in terms of internal coordinates] induces about 10% difference in the moment and up to 20% in the exchange interactions [30]. The same order of sensitivity was also reported for CaFe₂As₂ [31]. Therefore the deviation of up to 8% for moments and 30% for major exchange interactions (J_{1a} and J_2) are not significant, and become much smaller if $z(\text{As})$ could be refined for each material. Taking this into account, we can say that the magnetic moments and exchange interactions are uniform throughout the materials considered here.

One of the most important quantities to understand the magnetism and possibly the superconducting mechanism in these materials is the ratio of $J_{1a}/2J_2$, which has so far not been measured or calculated. According to the spin Hamiltonian models [21–23], assuming Fe pnictides as magnetic Mott insulators like cuprates, at $J_{1a}/2J_2 \approx 1$ the system is close to the quantum critical regime, so a superconducting ground state may appear as a result of the magnetic fluctuation [21–23,43,44]. Note that the calculated ratios shown in Table I are all around unity, demonstrating that this universal behavior of $J_{1a}/2J_2$ can arise from itinerant magnetism, without the system being close to a Mott transition. The deviations of $J_{1a}/2J_2$ from unity reflect not only the intrinsic material properties but also the sensitive dependence on $z(\text{As})$. Although there is no apparent relation between the $J_{1a}/2J_2$ ratio and T_C , the universal feature of $J_{1a}/2J_2$ near unity is closely associated to superconductivity since it is present throughout the materials studied here. The connection between itinerant AFM and superconductivity has been discussed previously [45].

Another important quantity is $|J_{1a} + 2J_2|$ which determines the spin-wave velocity in the $(\pi, 0)$ direction, and can be directly probed by neutron scattering experiments. The available experimental data are in general agreement with our calculation. For SrFe₂As₂ calculation shows $|J_{1a} + 2J_2| = 74 \text{ meV}$, not much smaller than the $100 \pm 20 \text{ meV}$ measured by neutron scattering [9]. Also, for CaFe₂As₂ our calculated $|J_{1a} + 2J_2| = 75 \text{ meV}$ is slightly smaller than the measured $95 \pm 16 \text{ meV}$ [26] (derived

from the observed spin-wave velocity; see equations below). Especially our result for BaFe₂As₂ is in good agreement with recent experiment by Ewings *et al.* [27]: One of their best fits shows that $J_{1a} = 36 \text{ meV}$, $J_2 = 18 \text{ meV}$, and $J_{1b} = -7 \text{ meV}$.

As an example, Fig. 3 shows the $z(\text{As})$ dependence of the magnetic moments and interactions of SrFe₂As₂. The moment is a simple monotonic function of $z(\text{As})$ ranging from $0.35\mu_B$ to $2.23\mu_B$. J_{1a} increases rapidly with $z(\text{As})$ at the beginning, saturates in the middle, and eventually turns down. This behavior is a result of the hybridization between Fe $d_{xz,yz}$ and As $p_{x,y}$ orbitals, as we discussed in the TB representation. Because of the shape and orientation of the Fe $d_{xz,yz}$ and As $p_{x,y}$ orbitals, there is a certain $z(\text{As})$ that gives the maximum overlapping, and hence largest J_{1a} . Note that J_{1b} changes sign at $z(\text{As})_{\text{exp}}$, and eventually surpasses J_2 . Also, J_{1a} and J_2 plateau in the small region around $z(\text{As})_{\text{exp}}$. Similar behaviors are also found in other materials. The $J_{1a}/2J_2$ and $|J_{1a} + 2J_2|$ values in Table I are robust against the small deviations in $z(\text{As})$ around the experimental values. From the data one can also calculate $J_{1a}/2J_2$ versus $z(\text{As})$, which reveals the existence of the “sweet spot” where the optimal ratio $J_{1a}/2J_2 = 1$ is achieved independent of any Heisenberg model assumption. In the case of SrFe₂As₂ it is $z(\text{As}) = 0.357$ (the inset of Fig. 3).

The calculated spin-wave dispersion gives more intuitive information about the magnetic interaction and anisotropy of these systems [9,25]. The dispersion relation of the 2D striped AFM lattice reads [46]

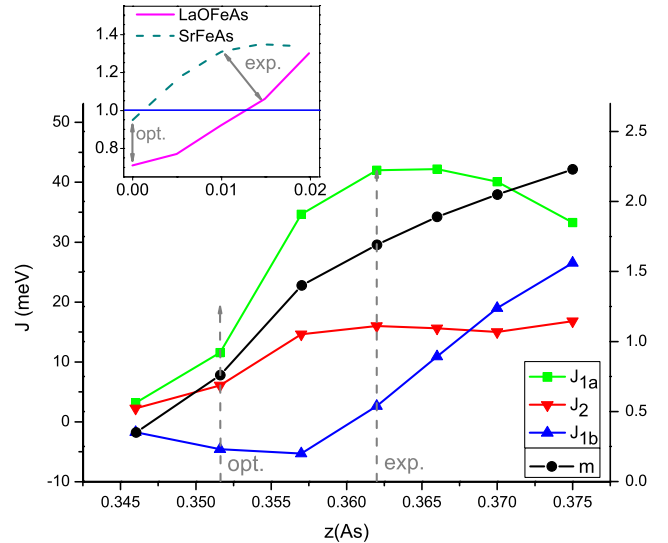


FIG. 3 (color online). Calculated magnetic moments (solid circles) and exchange interactions (squares and triangles) versus $z(\text{As})$ for SrFe₂As₂. The inset shows the calculated $J_{1a}/2J_2$ for SrFe₂As₂ (dashed line) and LaFeAsO (solid curve) as a function of $z(\text{As})$ given by the internal coordinates. The arrows point to the experimental value (exp.) and theoretically optimized value (opt.) of $z(\text{As})$. In the inset figure, the LDA-optimized $z(\text{As})$ is set to be zero reference.

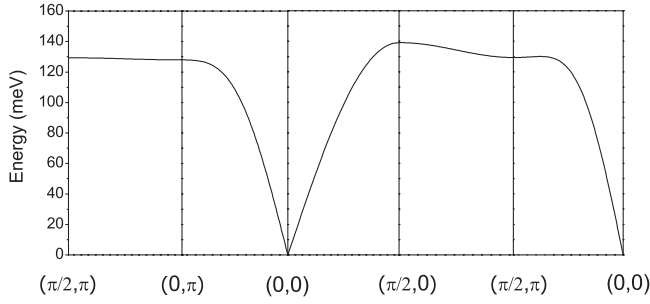


FIG. 4. The calculated spin-wave dispersion of SrFe₂As₂ along high-symmetry lines, the exchange constants are given in Table I.

$$\omega(\mathbf{q}) = S\sqrt{(\mathcal{J}_0 + J_{1b}(\mathbf{q}))^2 - (J_{1a}(\mathbf{q}) + J_2(\mathbf{q}))^2}. \quad (1)$$

Using the calculated magnetic exchange constants, we plot the spin-wave dispersion of SrFe₂As₂ in Fig. 4, whose $S = 0.94$ is taken from experiment [8]. The nonsymmetric dispersions in $(0, 0) - (0, \pi)$ and $(0, 0) - (\pi, 0)$ directions indicate in-plane magnetic anisotropy, which is a major difference from cuprates. At small q near $(0, 0)$, the spin-wave velocity in the $(\pi, 0)$ direction is $v_{\perp} = 2aS|J_{1a} + 2J_2|$, which is the relation used to experimentally determine $|J_{1a} + 2J_2|$, such as for SrFe₂As₂ [9]. The difference in J_{1a} and J_{1b} , a direct consequence of the Q_M -AFM ordering that breaks in-plane symmetry, accounts for the anisotropy in $(\pi, 0)$ and $(0, \pi)$ directions.

To conclude, we have studied magnetic exchange interactions in the various Fe-based high- T_C superconductors using first-principle based linear response calculations. The magnetic interactions can be well described by the first and second nearest-neighboring interactions. Importantly, $J_1/2J_2$ is close to unity for all the cases, just as would be the case for the frustration limit of a local moment model. Calculated spin-wave dispersions show the magnetic anisotropy and the roles of the three in-plane exchange interactions. Our result strongly suggests the magnetic fluctuation as the pairing mechanism for the superconducting ground state.

The authors would like to thank Elihu Abrahams (Rutgers Univ.) and Rajiv Singh (UC Davis) for helpful discussion on the spin wave dispersion. The authors acknowledge support from NSF Grant No. DMR-0606498 (S. Y. S) and DOE Grant No. DE-FG02-04ER46111 (W. E. P), and collaborative work supported by DOE SciDAC Grants No. SE-FC02-06ER25793 and No. DE-FC02-06ER25794.

- [1] Y. Kamihara *et al.*, J. Am. Chem. Soc. **130**, 3296 (2008).
 [2] X. H. Chen *et al.*, Nature (London) **453**, 761 (2008).
 [3] Z. A. Ren *et al.*, Chin. Phys. Lett. **25**, 2215 (2008).
 [4] J. H. Tapp *et al.*, Phys. Rev. B **78**, 060505(R) (2008).
 [5] C. Krellner *et al.*, Phys. Rev. B **78**, 100504(R) (2008).

- [6] A. Jesche *et al.*, Phys. Rev. B **78**, 180504(R) (2008).
 [7] A. I. Goldman *et al.*, Phys. Rev. B **78**, 100506(R) (2008).
 [8] J. Zhao *et al.*, Phys. Rev. B **78**, 140504(R) (2008).
 [9] J. Zhao *et al.*, Phys. Rev. Lett. **101**, 167203 (2008).
 [10] L. Zhao *et al.*, Chin. Phys. Lett. **25**, 4402 (2008).
 [11] F.-C. Hsu *et al.*, Proc. Natl. Acad. Sci. U.S.A. **105**, 14 262 (2008).
 [12] M. H. Fang *et al.*, Phys. Rev. B **78**, 224503 (2008).
 [13] K.-W. Yeh *et al.*, Europhys. Lett. **84**, 37 002 (2008).
 [14] Y. Mizuguchi *et al.*, Appl. Phys. Lett. **93**, 152505 (2008).
 [15] L. Boeri, O. V. Dolgov, and A. A. Golubov, Phys. Rev. Lett. **101**, 026403 (2008).
 [16] K. Haule, J. H. Shim, and G. Kotliar, Phys. Rev. Lett. **100**, 226402 (2008).
 [17] A. J. Drew *et al.*, Phys. Rev. Lett. **101**, 097010 (2008).
 [18] W. Bao *et al.*, arXiv:0809.2058.
 [19] J. J. Pulikotil, M. van Schilfhaarde, and V. P. Antropov, arXiv:0809.0283.
 [20] F. Ma *et al.*, arXiv:0809.4732.
 [21] Q. Si and E. Abrahams, Phys. Rev. Lett. **101**, 076401 (2008).
 [22] C. Fang *et al.*, Phys. Rev. B **77**, 224509 (2008).
 [23] C. Xu, M. Müller, and S. Sachdev, Phys. Rev. B **78**, 020501(R) (2008).
 [24] J. Wu, P. Phillips, and A. H. Castro Neto, Phys. Rev. Lett. **101**, 126401 (2008).
 [25] G. S. Uhrig *et al.*, arXiv:0810.3068 [Phys. Rev. B (to be published)].
 [26] R. J. McQueeney *et al.*, Phys. Rev. Lett. **101**, 227205 (2008).
 [27] R. A. Ewings *et al.*, Phys. Rev. B **78**, 220501(R) (2008).
 [28] A. Georges *et al.*, Rev. Mod. Phys. **68**, 13 (1996).
 [29] G. Kotliar *et al.*, Rev. Mod. Phys. **78**, 865 (2006).
 [30] Z. P. Yin *et al.*, Phys. Rev. Lett. **101**, 047001 (2008).
 [31] T. Yildirim, Phys. Rev. Lett. **102**, 037003 (2009).
 [32] K. Kuroki *et al.*, Phys. Rev. Lett. **101**, 087004 (2008).
 [33] C. Cao, P. J. Hirschfeld, and H.-P. Cheng, Phys. Rev. B **77**, 220506(R) (2008).
 [34] K. Nakamura, R. Arita, and M. Imada, J. Phys. Soc. Jpn. **77**, 093711 (2008).
 [35] E. Manousakis *et al.*, Phys. Rev. B **78**, 205112 (2008).
 [36] D. J. Singh and M.-H. Du, Phys. Rev. Lett. **100**, 237003 (2008).
 [37] A. I. Liechtenstein *et al.*, J. Magn. Magn. Mater. **67**, 65 (1987); P. Bruno, Phys. Rev. Lett. **90**, 087205 (2003).
 [38] X. Wan, Q. Yin, and S. Y. Savrasov, Phys. Rev. Lett. **97**, 266403 (2006).
 [39] M. J. Han, X. Wan, and S. Y. Savrasov, Phys. Rev. B **78**, 060401 (2008).
 [40] S. Y. Savrasov, Phys. Rev. B **54**, 16 470 (1996).
 [41] D. H. Lu *et al.*, Nature (London) **455**, 81 (2008).
 [42] I. I. Mazin and M. D. Johannes, Nature Phys. **5**, 141 (2009).
 [43] T. Yildirim, Phys. Rev. Lett. **101**, 057010 (2008).
 [44] A. V. Chubukov, D. V. Efremov, and I. Eremin, Phys. Rev. B **78**, 134512 (2008).
 [45] T. Moriya, Proc. Jpn. Acad. Ser. B **82**, 1 (2006).
 [46] Where $J_{1a}(\mathbf{q}) = 2J_{1a} \cos q_x$, $J_2(\mathbf{q}) = 2J_2[\cos(q_x + q_y) + \cos(q_x - q_y)]$, $J_{1b}(\mathbf{q}) = 2J_{1b} \cos q_y$, and $\mathcal{J}_0 = 2J_{1a} + 4J_2 - 2J_{1b}$.